

# A numerical procedure for the determination of elastic parameters in an incompressible solid

Adair R. Aguiar, Edmar B. T. Prado

*Department of Structural Engineering - SET/EESC/USP,  
São Carlos/SP – Brazil*

## Abstract

A class of plane problems related to the determination of the shear elastic modulus  $\mu$  of biological tissues is presented. A non-iterative numerical procedure to obtain approximate solutions to these problems from known displacement fields is employed. The displacement fields are obtained from quasi-static experiments that are possible to reproduce in laboratory and are simulated numerically using the Finite Element Method. Results for the distribution of  $\mu$  in a long cylinder of rectangular cross-section containing either an eccentric circular inclusion or an inclusion with a complex geometry are presented. This work is of great interest in the detection of cancerous tumors and in the differential diagnosis of biological tissues.

Keywords: Biomechanics, incompressibility, elasticity, Finite Element Method.

## 1 Introduction

It is known from experimental observations that abnormal biological tissues have different mechanical behavior than normal biological tissues [1]. In particular, Krouskop *et al.* [2] observe that abnormal tissues are stiffer than normal tissues. To quantify these observations, we consider biological tissues undergoing small deformations during quasi-static experiments and model these tissues isotropic, incompressible, and linearly elastic materials [3]. We are then interested on the determination of the shear elastic modulus  $\mu$  everywhere inside the elastic body.

The determination of elastic properties of biological tissues from experimental data has been the subject of intense investigation in recent years. See, for instance, Park and Maniatty [4] and references cited therein. Recently, Barbone and Gokhale [5] have considered plane problems in linear elastostatics and have shown that, except for four arbitrary constants, the general expression for the shear elastic modulus of an isotropic and incompressible material can be determined from two compatible and linearly independent displacement fields, which can be obtained from two distinct experiments. The arbitrary constants can be determined from the knowledge of the shear elastic modulus in four distinct points inside the body. The authors assume that both displacement fields are differentiable.

In this work, we propose a methodology to determine  $\mu$  from two linearly independent displacement fields with less restrictive assumptions. Our methodology does not require both any *a priori* knowledge of  $\mu$  inside the body and differentiability of the displacement fields. The methodology uses a Finite Element Method (FEM) to construct a numerical approximation for  $\mu$  inside an isotropic, incompressible, and linearly elastic body in equilibrium that is also in a state of plane strain.

## 2 The problem statement

Consider a long cylinder in a state of plane strain parallel to its bases and let  $\mathcal{B}$  be the undistorted natural reference configuration of a cross section of the cylinder. Points  $\mathbf{x} \in \mathcal{B}$  are mapped to points  $\mathbf{y}(x) = \mathbf{x} + \mathbf{u}(x)$ , where  $\mathbf{u}$  is the displacement field, which is assumed to be known in  $\mathcal{B}$  together with its boundary  $\partial\mathcal{B}$ . Park and Maniatty [4] present a brief discussion about different experimental techniques that can be used to measure the displacement of a point inside the body.

The cylinder undergoes a small deformation and is in equilibrium in the absence of body force, so that

$$\operatorname{div} \mathbf{T}(\mathbf{x}) = 0, \quad \forall \mathbf{x} \in \mathcal{B}, \quad (1)$$

where  $\mathbf{T}$  is the stress tensor. We assume that the body is incompressible, isotropic, and linearly elastic, so that

$$\mathbf{T} = -\pi \mathbf{1} + 2\mu \mathbf{E}, \quad (2)$$

where  $\pi$  is a constraint reaction field,  $\mu$  is the shear elastic modulus, which may depend on  $\mathbf{x} \in \mathcal{B}$ , and

$$\mathbf{E} = \nabla_s \mathbf{u} \equiv \frac{1}{2} [\nabla \mathbf{u} + (\nabla \mathbf{u})^T] \quad (3)$$

is the infinitesimal strain tensor. Observe from (2) that  $\mathbf{T}$  is determined from both the strain tensor  $\mathbf{E}$  and an arbitrary tensor  $-\pi \mathbf{1}$ , which represents the reaction of the body to local changes of volume. For incompressible materials, any infinitesimal deformation of  $\mathcal{B}$  must satisfy

$$\operatorname{tr} \mathbf{E} = \operatorname{div} \mathbf{u} = 0. \quad (4)$$

Substituting both (2) and (3) into (1), we obtain

$$-\nabla \pi(\mathbf{x}) + 2 \operatorname{div}(\mu \mathbf{E})(\mathbf{x}) = 0, \quad \forall \mathbf{x} \in \mathcal{B}. \quad (5)$$

We then consider the *inverse problem* of determining both the shear elastic modulus  $\mu : \mathcal{B} \rightarrow \mathbb{R}^2$  and the pressure field  $\pi : \mathcal{B} \rightarrow \mathbb{R}^2$  that satisfy the partial differential equation (5), where the displacement field  $\mathbf{u} : \mathcal{B} \rightarrow \mathbb{R}^2$  is known everywhere in  $\bar{\mathcal{B}} \equiv \mathcal{B} \cup \partial\mathcal{B}$  and satisfies the kinematical constraint (4).

Barbone and Gokhale [5] and McLaughlin and Yoon [6] show that, in general, the inverse problem stated above does not have a unique solution. Barbone and Gokhale [5] show, however, that by knowing

two compatible, linearly independent, and differentiable displacement fields from two experiments performed on the same body in a state of plane strain, the general expression of  $\mu$  contains at most four arbitrary constants. We review these results below with an example and propose a procedure to compute the arbitrary constants that can be extended to the more general case of  $\mu$  not being continuous.

## 2.1 Considerations about Uniqueness

Let  $(\mathbf{e}_1, \mathbf{e}_2, \mathbf{e}_3)$  be an orthonormal basis in  $\mathbb{R}^3$  associated to a system of rectangular cartesian coordinates with the origin in  $O$ . The vectors  $\mathbf{e}_1, \mathbf{e}_2$  are parallel to the plane that contains  $\mathcal{B}$  and  $\mathbf{e}_3$  is parallel to the axis of the straight cylinder. In this coordinate system, a point is represented by  $\mathbf{x} + \xi_3 \mathbf{e}_3$ , where  $\mathbf{x} = \xi_1 \mathbf{e}_1 + \xi_2 \mathbf{e}_2 \in \mathcal{B}$  and  $\xi_i \in \mathbb{R}$ ,  $i = 1, 2, 3$ . In addition,  $\mathbf{u} = v_1 \mathbf{e}_1 + v_2 \mathbf{e}_2$ , where  $v_i \in \mathbb{R}$ ,  $i = 1, 2$ . It follows from (3) that  $\mathbf{E} = \sum_{i,j=1}^2 \varepsilon_{ij} \mathbf{e}_i \otimes \mathbf{e}_j$ , where  $\mathbf{e}_i \otimes \mathbf{e}_j$  is the tensorial product between  $\mathbf{e}_1$  and  $\mathbf{e}_2$ , which is defined by  $(\mathbf{e}_i \otimes \mathbf{e}_j) \mathbf{e}_k = \delta_{jk} \mathbf{e}_i$ , and  $\varepsilon_{ij} \equiv \frac{1}{2} \left( \frac{\partial v_i}{\partial \xi_j} + \frac{\partial v_j}{\partial \xi_i} \right)$ . Since the cylinder is under plane strain, it follows from (4) that  $\varepsilon_{22} = -\varepsilon_{11}$ .

Taking the curl of (5) and assuming that  $\mathbf{u}$  is known everywhere in  $\mathcal{B}$ , we eliminate  $\pi$  and obtain the second-order differential equation

$$L[\mu] \equiv \left( \frac{\partial^2}{\partial \xi_1^2} - \frac{\partial^2}{\partial \xi_2^2} \right) (\mu \varepsilon_{12}) - 2 \frac{\partial^2}{\partial \xi_1 \partial \xi_2} (\mu \varepsilon_{11}) = 0 \quad (6)$$

where  $L[\mu]$  is a linear operator on  $\mu$ . Since  $(\varepsilon_{11})^2 + (\varepsilon_{12})^2 > 0$ , it is a standard procedure to show that  $L$  is hyperbolic [7] and that the characteristics of  $L$  are parallel and perpendicular to the principal directions of  $\mathbf{E}$ .

To illustrate the fact that  $\mu$  can not be determined from Eq. (6) alone and to motivate the introduction of a weak formulation of the inverse problem in Eq. (5) that leads to the determination of  $\mu$ , consider an isotopic, incompressible, and linearly elastic cylinder with square cross section in a state of plane strain perpendicular to its axis. The length of a side of the square section is  $\xi$ . The cylinder is subjected to two experiments that yield the homogeneous deformation fields

$$\varepsilon_{11}^1(\xi_1, \xi_2) = -\varepsilon_{22}^1(\xi_1, \xi_2) = \varepsilon_1, \quad \varepsilon_{12}^1(\xi_1, \xi_2) = 0, \quad (\text{Bi-axial experiment}), \quad (7)$$

$$\varepsilon_{11}^2(\xi_1, \xi_2) = \varepsilon_{22}^2(\xi_1, \xi_2) = 0, \quad \varepsilon_{12}^2(\xi_1, \xi_2) = \varepsilon_2, \quad (\text{Shearing experiment}). \quad (8)$$

In the bi-axial experiment, the cylinder is being pulled in one direction while being compressed in the other direction. The resultant forces on both sides have normal components of intensity  $\tau_1$ . In the shearing experiment, the same cylinder is subjected to tangential forces of intensity  $\tau_2$  on its lateral sides. Clearly, the deformation fields (7) and (8) satisfy the constraint (4) identically and, if  $\varepsilon_1 = \varepsilon_2$ , refer to the same state of simple shear. In this case, the principal directions, and hence the characteristics of  $L$  in (6), are inclined with respect to each other by an angle of 45 degrees.

Substituting the deformation fields (7) into (6) and solving for  $\mu$ , we obtain

$$\mu(\xi_1, \xi_2) = \phi_1(\xi_1) + \phi_2(\xi_2) \quad (9)$$

where  $\phi_i$ ,  $i = 1, 2$ , are arbitrary functions of its arguments, which can not be determined from the bi-axial experiment alone. To determine these functions, we substitute (5) together with the deformation fields (8) into (6). We then get

$$\mu(\xi_1, \xi_2) = \mu_0 + \mu_1\xi_1 + \mu_2\xi_2 + \mu_3(\xi_1^2 + \xi_2^2) \quad (10)$$

where  $\mu_i \in \mathbb{R}$ ,  $i = 0, \dots, 3$ , are arbitrary constants. The expression (10) is presented by Barbone and Gokhale [5] to illustrate the fact that, except for four arbitrary constants,  $\mu$  can be determined from two compatible and linearly independent displacement fields, which yield the deformation fields given by (7) and (8).

Corresponding to the deformation fields in both (7) and (8), there exist pressure fields  $\pi^1$  and  $\pi^2$  that can be determined from the substitution of (10) together with either (7) or (8) into (5), yielding

$$\pi^1(\xi_1, \xi_2) = 2\varepsilon_1 [\mu_1\xi_1 - \mu_2\xi_2 + \mu_3(\xi_1^2 - \xi_2^2) + \hat{\pi}^1] \quad (11)$$

$$\pi^2(\xi_1, \xi_2) = 2\varepsilon_2 [\mu_2\xi_1 + \mu_1\xi_2 + 2\mu_3\xi_1\xi_2 + \hat{\pi}^2] \quad (12)$$

where  $\hat{\pi}^i \in \mathbb{R}$ ,  $i = 1, 2$ , are arbitrary constants of integration.

To determine the constants  $\mu_i \in \mathbb{R}$ ,  $i = 0, \dots, 3$ , in (10) and  $\hat{\pi}^i \in \mathbb{R}$ ,  $i = 1, 2$ , in (11) and (12), we assume that the resultant forces  $\tau_i$ ,  $i = 1, 2$ , are known from experimental measurements. Since the traction field on the boundary is given by  $\mathbf{t}(\mathbf{x}, \mathbf{n}) = \mathbf{T}(\mathbf{x})\mathbf{n}$ , where  $\mathbf{n}$  is the outward normal to the boundary at  $\mathbf{x} \in \partial\mathcal{B}$  and  $\mathbf{T}$  is given by (2), we obtain a system of equations for the determination of the constants above. Even though this system is over-determined, we obtain the solution

$$2\mu_0\bar{\xi} = \frac{\tau_2}{\varepsilon_2} = \frac{\tau_1}{\varepsilon_1}, \quad \mu_1 = \mu_2 = \mu_3 = 0, \quad \hat{\pi}^1 = \hat{\pi}^2 = 0. \quad (13)$$

It then follows from (10) - (12) that  $\mu$  is constant, which means that the cylinder is homogeneous, and that  $\pi^i = 0$ ,  $i = 1, 2$ .

The procedure outlined above for the determination of  $\mu$  from both known deformation fields (7) and (8) and known resultant forces acting on complementary parts of the boundary of the cylinder can be extended to the general case of a non-homogeneous cylinder for which  $\mu$  may not even be continuous. In this case, the determination of the fields  $\mu$  e  $\pi^i$ ,  $i = 1, 2$ , is not trivial and requires the use of numerical methods that allow the construction of approximations to these fields. Below, we present a weak formulation of the inverse problem for the determination of  $\mu$  and  $\pi^i$ ,  $i = 1, 2$ , which together with a Finite Element Method allow the construction of these approximations.

## 2.2 The weak formulation of the inverse problem

Let  $\mathbf{u}^1$  and  $\mathbf{u}^2$  be two compatible and linearly independent displacement fields (see [5]), which are not necessarily differentiable and are obtained from two distinct experiments performed on the same body, and let

$$\mathbf{R}_i^j = \int_{\partial_i \mathcal{B}} \left( -\pi^j \mathbf{1} + 2\mu \nabla_s \mathbf{u}^j \right) \mathbf{n}_i dL \quad (14)$$

be resultant forces that are known on  $r$  complementary parts  $\partial_i \mathcal{B}$ ,  $i = 1, \dots, r$ , of  $\partial \mathcal{B}$ , so that  $\partial \mathcal{B} \equiv \bigcup_{i=1}^r \partial_i \mathcal{B}$  and  $\partial_i \mathcal{B} \cap \partial_j \mathcal{B} \neq \emptyset$ ,  $i \neq j$ . In (6),  $\pi^j$ ,  $j = 1, 2$ , is the pressure field associated with the displacement field  $\mathbf{u}^j$  and  $\mathbf{n}_i$  is a unit normal to  $\partial_i \mathcal{B}$ . To satisfy the global equilibrium condition, we must have  $\sum_{i=1}^r \mathbf{R}_i^j = 0$ ,  $j = 1, 2$ .

We want to determine the shear elastic modulus  $\mu : \mathcal{B} \rightarrow \mathbb{R}^2$  and the pressure field  $\pi^j : \mathcal{B} \rightarrow \mathbb{R}^2$ ,  $j = 1, 2$ , that satisfy both

$$-\nabla \pi^j(\mathbf{x}) + 2 \operatorname{div} (\mu \nabla_s \mathbf{u}^j)(\mathbf{x}) = 0, \quad \forall \mathbf{x} \in \mathcal{B} \quad (15)$$

and the expression (14) for known resultants  $\mathbf{R}_i^j$ , where the displacement field  $\mathbf{u}^j : \mathcal{B} \rightarrow \mathbb{R}^2$ ,  $j = 1, 2$ , is known everywhere in  $\overline{\mathcal{B}}$  and satisfy the kinematical constraint  $\operatorname{div} \mathbf{u}^j = 0$ .

Now, let  $\mathcal{L}^2(\mathcal{B})$  be the set of all square-integrable functions given by

$$\mathcal{L}^2(\mathcal{B}) = \{ \varphi : \mathcal{B} \rightarrow \mathbb{R}; |\varphi|_0 < \infty \} \quad (16)$$

where the norm  $|\bullet|_0$  is given by  $|\varphi|_0 \equiv \left( \int_{\mathcal{B}} |\varphi|^2 dA \right)^{1/2}$ , and let  $(\mathcal{H}^1(\mathcal{B}))^2$  be a Hilbert space defined by

$$(\mathcal{H}^1(\mathcal{B}))^2 = \{ \mathbf{v} : \mathcal{B} \rightarrow \mathbb{R}^2; \|\mathbf{v}\|_1 < \infty \} \quad (17)$$

where the norm  $\|\bullet\|_1$  is given by  $\|\mathbf{v}\|_1 \equiv \left( \int_{\mathcal{B}} (\mathbf{v} \cdot \mathbf{v} + \nabla \mathbf{v} \cdot \nabla \mathbf{v}) dA \right)^{1/2}$ . Here, a displacement field  $\mathbf{u} \in (\mathcal{H}^1(\mathcal{B}))^2$  is kinematically admissible if it satisfies  $\mathbf{u} = \bar{\mathbf{u}}$  on  $\partial \mathcal{B}$ , where  $\bar{\mathbf{u}}$  is known on the boundary  $\partial \mathcal{B}$ , and  $\mathbf{v} \in (\mathcal{H}^1(\mathcal{B}))^2$  is an admissible variation if it satisfies  $\mathbf{v} = \mathbf{0}$  on  $\partial \mathcal{B}$ . We then introduce  $\mathcal{S}$  as the set of all admissible displacements and  $\mathcal{V}$  as the set of all admissible variations.

The weak form of the inverse problem that we shall consider in this work consists of finding  $\mu \in \mathcal{L}^2(\mathcal{B})$  and  $\pi^j \in \mathcal{L}^2(\mathcal{B})$ ,  $j = 1, 2$ , that satisfy

$$-\int_{\mathcal{B}} \pi^j \operatorname{tr} \nabla_s \mathbf{v} dA + 2 \int_{\mathcal{B}} \mu \nabla_s \mathbf{u}^j \cdot \nabla_s \mathbf{v} dA = 0, \quad \mathbf{u}^j \in \mathcal{S}, \quad j = 1, 2, \quad \forall \mathbf{v} \in \mathcal{V}, \quad (18)$$

together with (14) for  $i = 1, \dots, r$ .

The weak form stated above together with a finite element methodology discussed in Aguiar and Prado [8] allow an approximate reconstruction of  $\mu$  from the given data  $\mathbf{u}^j$  and  $\mathbf{R}_i^j$ ,  $j = 1, 2$ ,  $i = 1, \dots, r$ . Observe that this formulation does not require differentiability of  $\mathbf{u}^j$ . In the next section, we review briefly the main results of the finite element methodology.

### 2.3 The discrete formulation of the inverse problem

We want to construct finite element approximations for the solution  $(\mu, \pi^1, \pi^2) \in (\mathcal{L}^2(\mathcal{B}))^3$  of the inverse problem given by (18) together with (14) for  $i = 1, \dots, r$ . For this, we consider a finite element formulation based on the introduction of discrete problems over finite-dimensional subsets of  $\mathcal{L}^2(\mathcal{B})$  and  $\mathcal{V}$ . The corresponding discrete problems can be solved using direct solvers, as opposed to iterative solvers used in the literature, such as in Park and Maniatty [4].

We begin by assuming that  $\mathcal{B} \in \mathbb{R}^2$  is a polygonal domain composed of  $m$  non-overlapping quadrilaterals  $\mathcal{K}_k \in \mathbb{R}^2$ ,  $k = 1, 2, \dots, m$ , so that

$$\mathcal{B} = \bigcup_{k=1}^m \mathcal{K}_k \quad (19)$$

and such that the intersection of any two of these quadrilaterals is either empty, a point, or, a straight line. For each  $\mathcal{K}_k \subset \mathcal{B}$ , the interior of the quadrilateral  $\mathcal{K}_k$  is non-empty.

Let  $\mathcal{K}_k \in \mathbb{R}^2$ ,  $k = 1, 2, \dots, m$ , be endowed with the set of nodes  $\mathbf{x}_{ki} \in \mathcal{K}_k$ ,  $i = 1, \dots, 4$ , which are the vertices of  $\mathcal{K}_k$ . We shall consider Lagrange finite elements  $(\mathcal{K}_k, \mathcal{P}_k, \Sigma_k)$ ,  $k = 1, \dots, m$ , where  $\mathcal{P}_k$  is a set of smooth functions  $\varphi : \mathcal{K}_k \rightarrow \mathbb{R}$  and  $\Sigma_k$  is a set of degrees of freedom corresponding to the coefficients  $\varphi(\mathbf{x}_{ki})$ . The functions  $\varphi$  are linear combinations of normalized basis functions  $\varphi_{ki}$ ,  $i = 1, \dots, 4$ , so that  $\varphi_{ki}(\mathbf{x}_{kj}) = \delta_{ij}$ . The functions  $\varphi_{ki}$ ,  $i = 1, \dots, 4$ , are continuous over  $\mathcal{K}_k$ . In this way, a finite element mesh is the union of all the finite elements  $(\mathcal{K}_k, \mathcal{P}_k, \Sigma_k)$ ,  $k = 1, \dots, m$ .

Let us denote as  $\mathcal{N} \equiv \{\mathbf{x}_1, \mathbf{x}_2, \dots, \mathbf{x}_n\} \in \mathcal{B}$  the complete set of  $n$  nodes in  $\mathcal{B}$ . Then, for each  $i = 1, \dots, m$ , and each  $k = 1, \dots, 4$ ,  $\mathbf{x}_{ki} \in \mathcal{K}_k$  corresponds to a unique element from  $\mathcal{N}$ . We define the set of functions  $\varphi_j : \mathcal{B} \rightarrow \mathbb{R}$ ,  $j = 1, \dots, n$ , such that  $\varphi_j(\mathbf{x}) = \varphi_{ki}(\mathbf{x})$  for  $\mathbf{x} \in \mathcal{K}_k$ . Thus,  $\varphi_j$  is continuous on  $\mathcal{B}$  and satisfies  $\varphi_j(\mathbf{x}_i) = \delta_{ij}$ ,  $i, j = 1, \dots, n$ . In fact, the set of functions  $\varphi_j$  is a finite-dimensional basis for the set of continuous functions defined by

$$\mathcal{P} = \left\{ \varphi : \mathcal{B} \rightarrow \mathbb{R} \mid \varphi(\mathbf{x}) = \sum_{j=1}^n \alpha_j \varphi_j(\mathbf{x}), \forall (\alpha_1, \alpha_2, \dots, \alpha_n) \in \mathbb{R}^n \right\} \quad (20)$$

We now define the finite-dimensional space  $\mathcal{V}_h$  as follows

$$\mathcal{V}_h = \left\{ \mathbf{v} \in (\mathcal{C}^0(\mathcal{B}_h))^2 : \mathbf{v} \in (\mathcal{P}(\mathcal{B}))^2, \mathbf{v} = \mathbf{0} \text{ on } \partial\mathcal{B} \right\} \quad (21)$$

where  $h$  stands for the characteristic length of the finite element mesh. Observe from (21) that  $\mathcal{V}_h \subset \mathcal{V}$ . A function  $\mathbf{v}_h \in \mathcal{V}_h$  has the representation

$$\mathbf{v}_h(\mathbf{x}) = \sum_{i=1}^{2n} \vartheta_i \mathbf{w}_i(\mathbf{x}), \quad \mathbf{x} \in \bar{\mathcal{B}}, \quad (22)$$

where  $\vartheta_i \in \mathbb{R}$  and  $\mathbf{w}_i$  is a vector in  $\mathbb{R}^2$  of the form

$$\mathbf{w}_{2i-1} = (\varphi_i, 0), \quad \mathbf{w}_{2i} = (0, \varphi_i), \quad i = 1, 2, \dots, n, \quad (23)$$

relative to a fixed orthonormal base, with  $\varphi_i$  being a scalar basis function defined for the  $i^{\text{th}}$  node in the set  $\mathcal{N}$  introduced above. In particular, notice that  $\mathbf{v}_h(\mathbf{X}_i) = (\vartheta_{2i-1}, \vartheta_{2i})$  for  $i = 1, 2, \dots, n$ . Each  $\vartheta_i$ ,  $i = 1, 2, \dots, 2n$ , is a degree of freedom associated with  $\mathcal{V}_h$ . Thus, considering the fact that each node in  $\mathcal{N}$  has two degrees of freedom and that  $\mathbf{v}_h \in \mathcal{V}_h$ , it is convenient to decompose the complete set of  $2n$  degrees of freedom into two complementary integer sets  $\mathcal{Z}^*$  e  $\mathcal{Z}$ , such that  $\vartheta_i = 0$ ,  $\forall i \in \mathcal{Z}^*$ , and  $\mathcal{Z} \equiv \{1, 2, \dots, n\} \setminus \mathcal{Z}^*$ .

Let us also define the space

$$\mathcal{L}_h^2 = \{\mu_h : \mathcal{B}_h \rightarrow \mathbb{R} : \mu_h \text{ is piecewise continuous on } \mathcal{B}_h\} \quad (24)$$

An element  $\mu_h \in \mathcal{L}_h^2$  has the representation

$$\mu_h(\mathbf{x}) = \sum_{k=1}^m \mu_k \tau_k(\mathbf{x}), \quad \mathbf{x} \in \bar{\mathcal{B}}, \quad (25)$$

where  $\mu_k \in \mathbb{R}$  and  $\tau_k$  is a scalar basis function, which is piecewise constant, has support in  $\mathcal{K}_k$ , and is normalized so that  $\varphi_j(\mathbf{x}) = \delta_{ij}$  for  $x \in \mathcal{K}_i$ ,  $i, j = 1, \dots, m$ .

Next, we assume that both fields  $\mathbf{u}^1$  and  $\mathbf{u}^2$  are known and use the representation given by Eq. (22) to approximate  $\mu$  and  $\pi^j$ ,  $j = 1, 2$ , in the form

$$\mu_h = \sum_{k=1}^m \mu_k \tau_k \quad \text{and} \quad \pi_h^i = \sum_{k=1}^m \pi_k^i \tau_k, \quad \mathbf{x} \in \bar{\mathcal{B}}, \quad (26)$$

where  $\mu_k \in \mathbb{R}$  and  $\pi_k^i \in \mathbb{R}$ ,  $i = 1, 2$ ,  $k = 1, 2, \dots, m$ . We also assume that  $\partial_j \mathcal{B} \subset \partial \mathcal{B}$  is given by

$$\partial_j \mathcal{B} = \bigcup_{p \in \mathcal{Z}_j} \mathcal{D}_p \quad (27)$$

where  $\mathcal{D}_p$  is a side of  $\mathcal{K}_p$  that also belongs to  $\partial \mathcal{B}$  and  $\mathcal{Z}_j$  is the set of integer numbers that identify the finite elements with sides contained in  $\partial_j \mathcal{B}$ .

Substituting the Eq. (26) and  $v_h$ , given by Eq. (22), into both Eq. (14) and Eq. (18), and using the fact that the coefficients  $\vartheta_i$ ,  $i \in \mathcal{Z}$ , are arbitrary, these equations can be rewritten as

$$\sum_{q=1}^{2m} \alpha_{pq}^j \omega_q^j = 0, \quad p \in \mathcal{Z}, \quad (28)$$

$$\sum_{q \in \mathcal{Z}_i} \beta_q^j \omega_q^j = \mathbf{R}_i^j, \quad i = 1, 2, \dots, r, \quad (29)$$

where  $j = 1, 2$ , and

$$\alpha_{p(2q-1)}^j = 2 \int_{\mathcal{K}_q} \nabla_s \mathbf{u}^j \cdot \nabla_s \mathbf{w}_p dA, \quad \alpha_{p(2q)}^j = - \int_{\mathcal{K}_q} \mathcal{K}_q \text{tr} \nabla_s \mathbf{w}_p dA, \quad (30)$$

$$\beta_{2q-1}^j = 2 \int_{\mathcal{D}_q} (\nabla_s \mathbf{u}^j) \mathbf{n}_q dA, \quad \beta_{2q}^j = - \int_{\mathcal{D}_q} \mathbf{n}_q dA, \quad (31)$$

$$\omega_{2q-1}^j = \mu_q, \quad \omega_{2q}^j = \pi_q^j. \quad (32)$$

Then, the discrete inverse problem associated to the problem given by Eq. (14) and Eq. (18) consists of finding the coefficients  $\omega_q^j, j = 1, 2, q = 1, \dots, m$ , defined by (32) that satisfy the linear system given by (28) - (31).

In general, the linear system given by (28) - (31) is over-determined. To solve this system, we use the Singular Value Decomposition algorithm presented by Golub and van Loan (1996). The main input data are the coefficients on the right side of both Eq. (28) and Eq. (29), the matrix  $\mathbf{W}$  formed by the coefficients that multiply  $\omega_q^j$  on the left side of these equations, the dimensions of  $\mathbf{W}$ , and a tolerance that yields the largest non-singular, square matrix of  $\mathbf{W}$ . Here, the tolerance is a non-negative number below which a singular value of  $\mathbf{W}$  is considered to be zero. A preliminary study of the influence of the tolerance on the values of the coefficients  $\mu_k, k = 1, \dots, m$  in Eq. (26) allows to conclude that, for tolerances below  $10^{-8}$ , all the values obtained for these coefficients were physically plausible and differed very little from each other.

### 3 Numerical results

We show in Fig. 1 a schematic representation of two experiments that yield both the resultants  $\mathbf{R}_i^j$  in (29) and the displacements  $\mathbf{u}^j$  in both (30) and (31). These experiments are carried out on a cylinder of square cross section containing an eccentric cylindrical inclusion of circular cross section. The length of a side of the square section is  $\xi = 50$  mm and the radius of the circular section is  $r = 6$  mm. The conditions on the boundary of the cylinder are the same ones considered for the experiments described in Section 2.1. Here, however, the resulting deformation fields are not homogeneous.

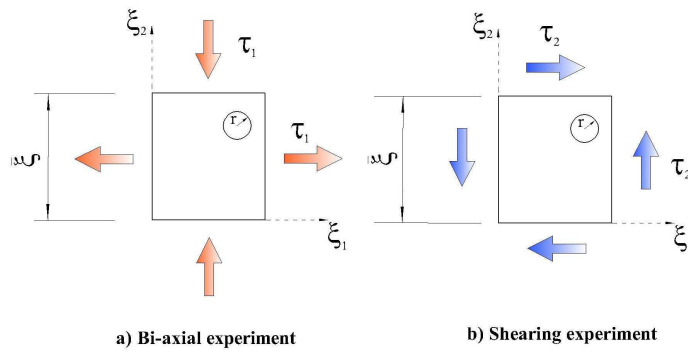


Figure 1: Bi-axial and shearing experiments on a cylinder containing an inclusion.

We have simulated numerically both experiments to obtain the resultant forces  $\mathbf{R}_i^j$  and the displacements  $\mathbf{u}^j$ . For this, we use the Finite Element package *Ansys 5.5*<sup>1</sup> and assumed that the shear elastic moduli of both the matrix, which is the cylinder without the inclusion, and the inclusion are given by, respectively,  $\mu_M = 36$  kPa and  $\mu_I = C_R \mu_M$ , where  $C_R \geq 0$  is the shear modulus contrast ratio. Observe that  $C_R = 0$  corresponds to an empty hole,  $C_R = 1$  corresponds to a homogeneous cylinder, and  $C_R > 1$  corresponds to an inclusion that is  $C_R$  times stiffer than the matrix. In Fig. 2 we show a mesh of finite elements used in the computation of both  $\mathbf{u}^j$  and  $\mathbf{R}_i^j$ , where the inclusion is shown on the upper right side. In these simulations we have also obtained approximations for the pressure fields  $\pi^j, j = 1, 2$ .

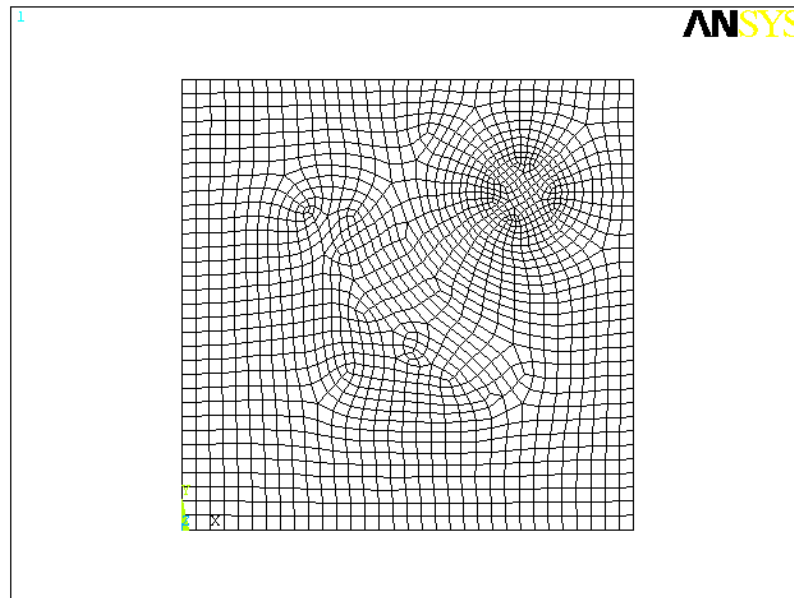


Figure 2: Non-uniform mesh of finite elements to discretize the square cross section of a cylinder containing an eccentric inclusion.

With the vectors  $\mathbf{u}^j$  and  $\mathbf{R}_i^j$  computed from the numerical simulations above, we have solved the system given by (28) - (32) using the non-uniform mesh of Fig. 2 and computed approximations for both  $\mu$  and  $\pi^j, j = 1, 2$ , from (26). We have verified that the approximations of  $\pi^j, j = 1, 2$ , are in very good agreement with the corresponding approximations obtained from the numerical simulations above.

<sup>1</sup>*Ansys 5.5* is proprietary software of Ansys Inc., USA.

In the next two figures we show sequences of frames that use color maps to represent the distribution of the shear elastic modulus inside the cylinder of square cross section. Each frame has its own color map, which corresponds to a range of values for  $\mu$ . The smallest and largest values of  $\mu$  correspond to the colors at, respectively, the bottom and the top of the color map. The frames on the upper left corner in both figures contain exact values of  $\mu$  and are used as reference frames to be compared with the other five frames. These five frames are obtained from different finite element meshes, which are represented in Tab. 1 by increasing numbers of nodes and elements. In particular, Fig. 2 corresponds to Mesh 5 in Tab. 1.

In Fig. 3 and Fig. 4 we consider the cases  $C_R = 0^2$  and  $C_R = 6$ , respectively. Comparing the reference frame (a) in each figure with the other five frames of the same figure and observing the values in the corresponding legend, we note that  $\mu_h$ , defined by (26.a), converges to  $\mu$  as the mesh is refined. In both cases,  $\mu_h \rightarrow 36$  kPa everywhere inside the matrix. Inside the inclusions, we see from Fig. 3 that  $\mu_h \rightarrow 0$  kPa and from Fig. 4 that  $\mu_h \rightarrow 216$  kPa.

Table 1: Finite element meshes for a cylinder with an eccentric inclusion.

Mesh	Number of nodes	Number of elements
1	733	668
2	931	866
3	1077	1012
4	1218	1153
5	1535	1470

Next, in Fig. 5 we consider an inclusion with a cross section having a complex geometry. The color maps of both Frame (a) and Frame (b) represent, respectively, the exact and the calculated values of  $\mu$  inside the inclusion and the matrix. By comparing both frames, we see that our numerical approach yields accurate values for  $\mu$  and is capable of reconstructing the geometry of the inclusion.

---

<sup>2</sup>Because of numerical difficulties experienced during the numerical simulations using ANSYS 5.5, we used  $C_R = 10^{-25}$  and Poisson's ratio  $\nu_I = 0.3$  for the inclusion, instead of  $C_R = 0$  and  $\nu_I = 0.5$ .

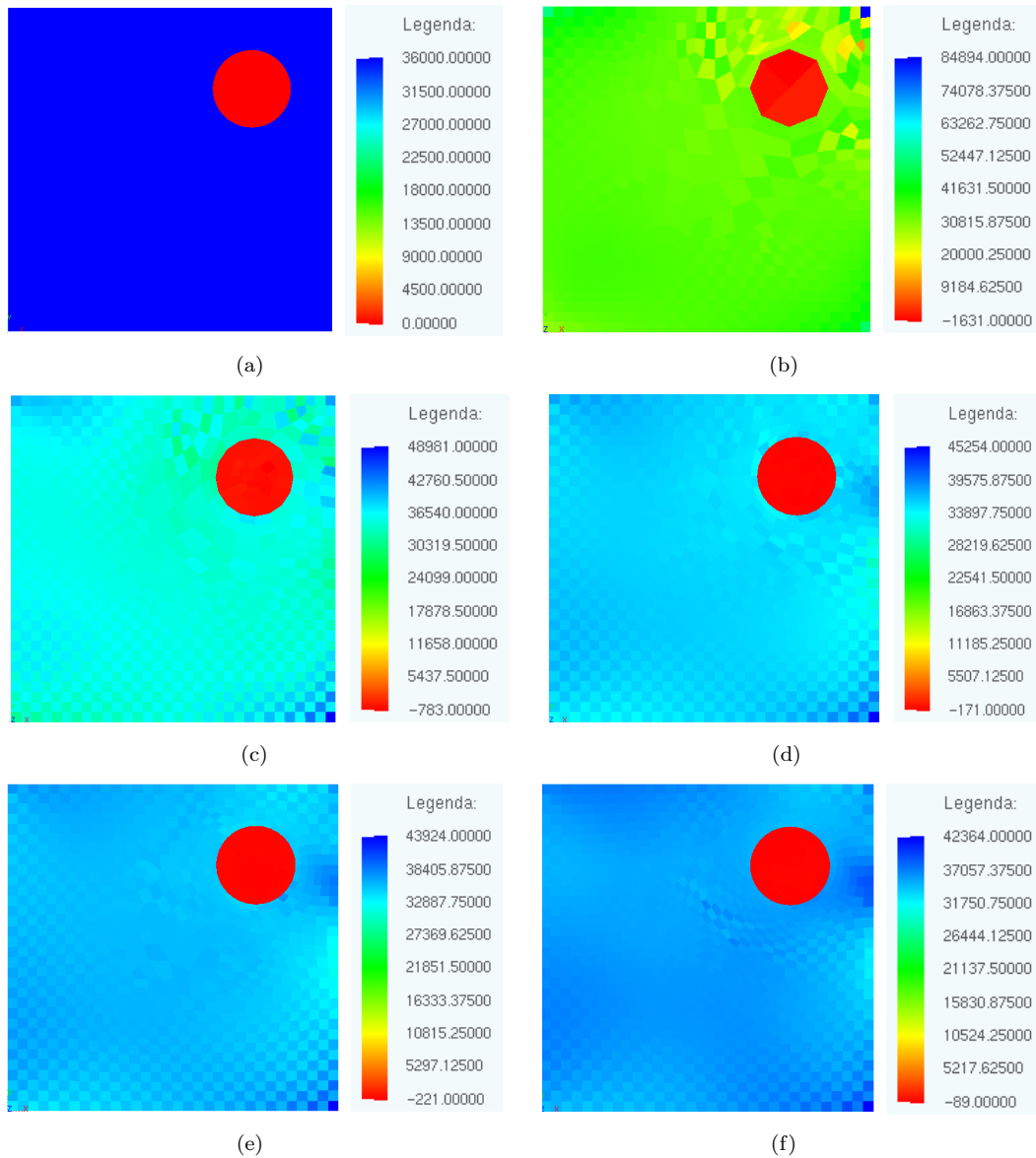


Figure 3: Reconstruction of  $\mu$  in a cylinder containing an eccentric circular hole, ( $C_R = 0$ ).

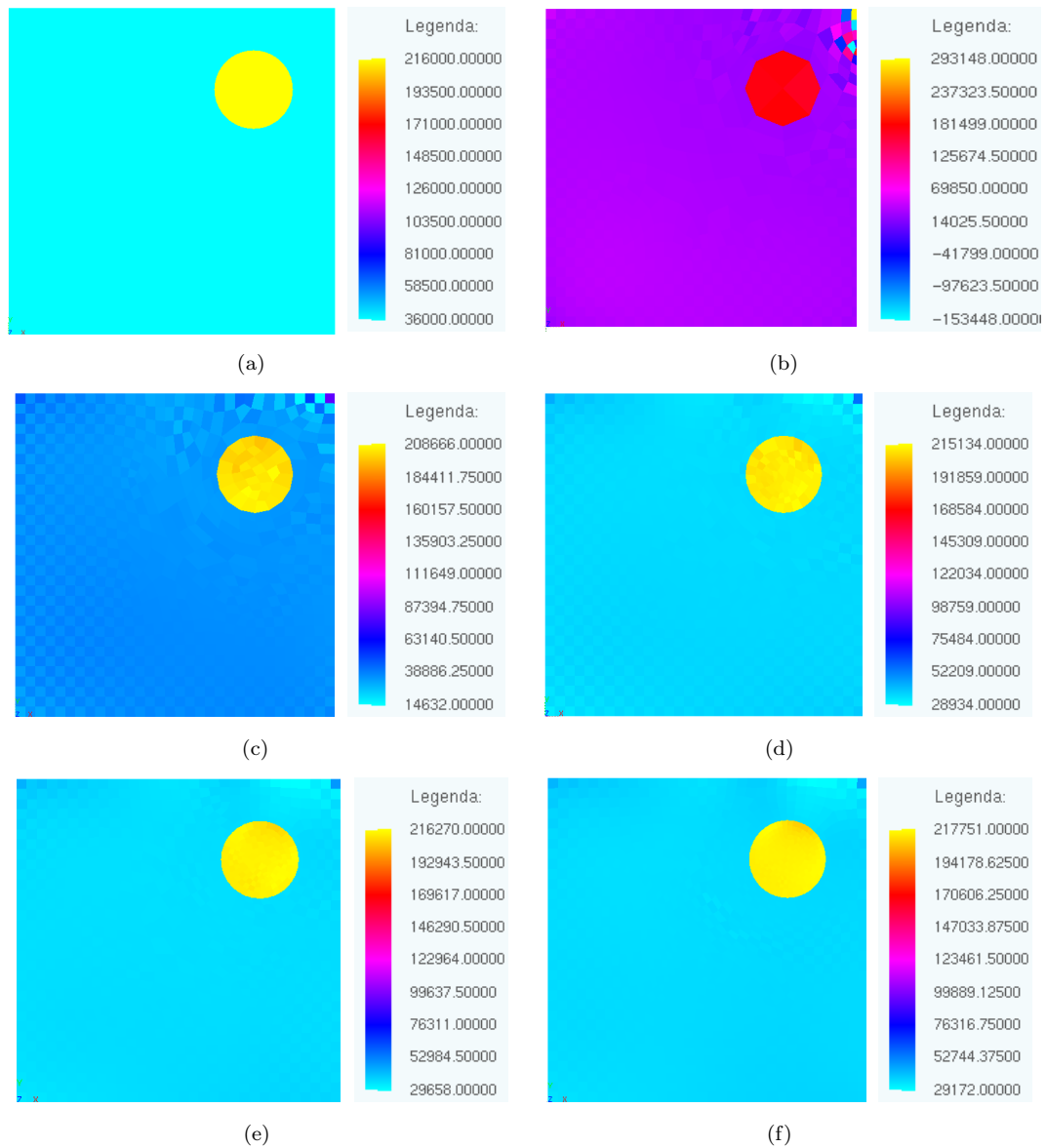


Figure 4: Reconstruction of  $\mu$  in a cylinder containing an eccentric circular inclusion with  $C_R = 6$ .

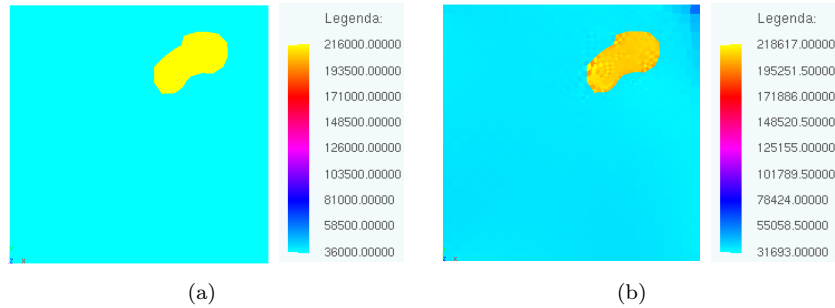


Figure 5: Reconstruction of  $\mu$  in a cylinder containing an inclusion with a complex geometry.

#### 4 Conclusion

The theoretical approach used in this work to reconstruct the shear elastic modulus  $\mu$  of an isotropic, incompressible, and linearly elastic solid in a state of plane strain together with the numerical method proposed in Aguiar and Prado [8], which is based on a Finite Element formulation described briefly in Section 2, yield very accurate results. In particular, these results are not sensitive to numerical errors due (i) numerical simulation of both experiments, which yield approximations to both  $\mathbf{u}^1$  and  $\mathbf{u}^2$  and to the corresponding resultant forces  $\mathbf{R}_i^1$  and  $\mathbf{R}_i^2$ ,  $i = 1, \dots, r$ ; (ii) finite element discretization of the inclusion, which has a non-polygonal geometry, using quadrilateral elements; (iii) use of finite elements to obtain the displacement fields  $\mathbf{u}^1$  and  $\mathbf{u}^2$  that may yield the locking effect, which appear in the numerical simulation of problems involving incompressible materials. See a discussion about this effect in Hughes [9].

We are now investigating the application of this numerical method (i) using regular meshes, instead of the non-uniform meshes used in this work; (ii) in the reconstruction of  $\mu$  in problems that are more general than plane problems; (iii) using constitutive relations that take into account viscous and nonlinear behavior of living tissues.

#### Acknowledgements

The authors wish to acknowledge CAPES (Coordination for the Improvement of High Education Personnel) for its support of this research.

#### References

- [1] Fung, Y.C., *Biomechanics: mechanical properties of living tissues*. Springer: New York, 2nd edition, 2004.
- [2] Krouskop, T.A., Wheeler, T.M., Kallel, F. & Garra, B.S.T., Elastic moduli of breast and prostate tissues under compression. *Ultrasound Imaging*, **4(20)**, pp. 260–274, 1998.
- [3] Mridha, M. & Ödman, S., Noninvasive method for the assessment of subcutaneous edema. *Med Biol Eng*

- Comput.* **24(4)**, pp. 393–398, 1986.
- [4] Park, E. & Maniatty, A.M., Shear modulus reconstruction in dynamic elastography: time harmonic case. *Physics in Medicine and Biology*, **(51)**, pp. 3697–3721, 2006.
  - [5] Barbone, P.E. & Gokhale, N.H., Elastic modulus imaging: on the uniqueness and nonuniqueness of the elastography inverse problem in two dimensions. *Inverse Problems*, **20**, pp. 283–296, 2004.
  - [6] McLaughlin, J.R. & Yoon, J.R., Unique identifiability of elastic parameters from time-dependent interior displacement measurement. *Inverse Problems*, **20**, pp. 25–45, 2004.
  - [7] Weinberger, H.F., *Partial differential equations with complex variables and transform methods*. John Wiley & Sons, Inc.: New York, USA, 1965.
  - [8] Aguiar, A.R. & Prado, E.B.T., A Finite Element Methodology to determine elastic parameters in biological tissues. *XXIX CILAMCE - Iberian Latin American Congress on Computational Methods in Engineering*, Maceió, 2008. University of Minnesota Supercomputing Institute Research Report UMSI 2008/100, September 2008 and CB number 2008-43.
  - [9] Hughes, T.J.R., *The Finite Element Method: Linear Static and Dynamic Analysis*. Prentice-Hall, Inc.: Englewood Cliffs, New Jersey, 1987.